University of Massachusetts Amherst

ScholarWorks@UMass Amherst

2020

Cavitation in soft matter

Christopher W. Barney

Carey E. Dougan

Kelly R. McLeod

Amir Kazemi-Moridani

Yue Zheng

See next page for additional authors

Authors

Christopher W. Barney, Carey E. Dougan, Kelly R. McLeod, Amir Kazemi-Moridani, Yue Zheng, Ziyu Ye, Sacchita Tiwari, Ipek Sacligil, Robert A. Riggelman, Shengqiang Cai, Jae-Hwang Lee, Shelly Peyton, Gregory N. Tew, and Alfred J. Crosby

PERSPECTIVE

Cavitation in soft matter

Christopher W. Barney[a,1], Carey E. Dougan[b,1], Kelly R. McLeod[a], Amir Kazemi-Moridani[c], Yue Zheng[d], Ziyu Ye[e], Sacchita Tiwari[c], Ipek Sacligil[a], Robert A. Riggleman[f,2], Shengqiang Cai[d,2], Jae-Hwang Lee[c,2], Shelly R. Peyton[b,2], Gregory N. Tew[a,2], and Alfred J. Crosby[a,2]

Cavitation is the sudden, unstable expansion of a void or bubble within a liquid or solid subjected to a negative hydrostatic stress. Cavitation rheology is a field emerging from the development of a suite of materials characterization, damage quantification, and therapeutic techniques that exploit the physical principles of cavitation. Cavitation rheology is inherently complex and broad in scope with wide-ranging applications in the biology, chemistry, materials, and mechanics communities. This perspective aims to drive collaboration among these communities and guide discussion by defining a common core of high-priority goals while highlighting emerging opportunities in the field of cavitation rheology. A brief overview of the mechanics and dynamics of cavitation in soft matter is presented. This overview is followed by a discussion of the overarching goals of cavitation rheology and an overview of common experimental techniques. The larger unmet needs and challenges of cavitation in soft matter are then presented alongside specific opportunities for researchers from different disciplines to contribute to the field.

soft solids | traumatic brain injury | TBI | rheology | bubble

Cavitation is the sudden, unstable expansion of a void or bubble within a liquid or solid subjected to a negative hydrostatic stress. While predominantly studied in fluids, cavitation is also an origin of damage in soft materials, including biological tissues. Examples of cavitation in fluids and soft solids are shown in Fig. 1 *A–C*. As one key example, strong evidence suggests that cavitation occurs in the brain during sudden impacts, leading to traumatic brain injury (TBI) (3). Research on this life-impacting injury and its relation to cavitation has accelerated in recent years (4–8). A broader and deeper understanding of cavitation within soft matter is necessary to navigate the complex paths that lead to damage in the brain and other soft materials.

Cavitation in fluids has been studied extensively since Rayleigh's (9) formulation in 1917, which predicted that the maximum pressure in a cavitating liquid is proportional to the far-field pressure and inversely proportional to the cavity size. As surface energy collapses a cavity, pressure near the cavity wall becomes large. In fact, some measurements have suggested that collapsing pressures can exceed 6 GPa for water or nearly the pressure needed to form diamond (10) Although direct measurements are challenging, evidence for the impact of cavitation-related forces, including damage and wear on engineered components and biological structures, is well documented (11).

In solids, cavitation can occur in the solid itself or in liquid phases within a solid, such as water within a swollen hydrogel or tissue. Whereas cavitation in liquids leads to damage on nearby solids on collapse, cavitation within solids can cause damage to the material and surroundings during both the expansion and collapse. Cavitation in solids has been documented since at least the 1930s; however, this process and related pathways to damage have received considerably less attention than cavitation in liquids (12, 13).

[a]Polymer Science & Engineering Department, University of Massachusetts, Amherst, MA 01003; [b]Department of Chemical Engineering, University of Massachusetts, Amherst, MA 01003; [c]Department of Mechanical & Industrial Engineering, University of Massachusetts, Amherst, MA 01003; [d]Department of Mechanical & Aerospace Engineering, University of California San Diego, La Jolla, CA 92093; [e]Department of Chemistry, University of Pennsylvania, Philadelphia, PA 19104; and [f]Department of Chemical & Biomolecular Engineering, University of Pennsylvania, Philadelphia, PA 19104

[1]C.W.B. and C.E.D. contributed equally to this work.

[2]To whom correspondence may be addressed. Email: rrig@seas.upenn.edu, shqcai@ucsd.edu, leejh@umass.edu, speyton@umass.edu, tew@mail.pse.umass.edu, or acrosby@umass.edu.
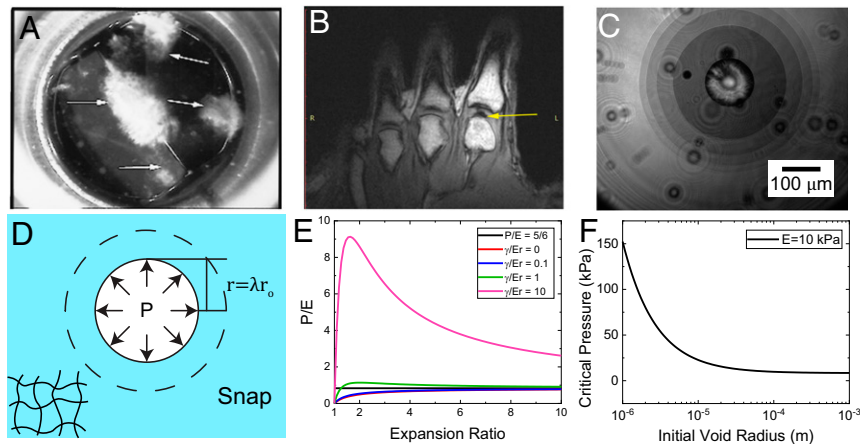
Fig. 1. (*A*) Example of cavitation in the wake of an artificial heart valve. Reprinted by permission from ref. 1 (Copyright 1999, Springer Nature: Annals of Biomedical Engineering,). (*B*) Example of cavitation in knuckles as they crack. Reprinted from ref. 2, which is licensed under CC BY 4.0. (*C*) Example of cavitation in a synthetic silicone on laser ablation. (*D*) Schematic of a spherical void of initial radius *r* in a gel that experiences an unstable snap from a low stretch state to a high stretch state at a critical pressure. (*E*) Pressure–expansion curves for voids with varying ratios of interfacial energy to elastic modulus. (*F*) Critical pressure against size scale for a hydrogel with a modulus similar to those reported for biological tissues.

The pathways to damage induced by cavitation in tissues and other soft materials are expected to be related. A quantitative understanding of how damage depends on the rate of cavity expansion and collapse and on the molecular and mesoscale structure will lead to improved predictions for injury detection and prevention in tissues. This understanding will also lead to the design of more sustainable materials that mitigate or prevent damage and new technologies that take advantage of the fast, expansive motions that can be associated with soft material cavitation. In this perspective, we provide a concise review of the mechanics and dynamics associated with cavitation in soft solids, describe current experimental methods to measure the effects of cavitation deformations on soft materials and tissues, highlight opportunities for new measurements using cavitation, and discuss unmet needs and challenges with regard to understanding cavitation in soft solids and tissues.

Cavitation Mechanics and Dynamics

Elasticity and Surface Energy Formulation for Cavitation. Failure in soft solids was linked to cavitation-like phenomena as early as the 1930s, while the relationship between the critical pressure for cavity expansion and the materials properties was not developed until the 1950s (12–15). Gent and coworkers (14, 15) related the pressure *P* within a spherical void in an infinitely thick, neo-Hookean material [e.g., rubber, hydrogels, liver (16), etc.] as sketched in Fig. 1*D* to its expansion, λ, and elastic modulus, *E* (14). A later modification added the resistance provided by the void's interfacial energy. Thus, the pressure equation is the superposition of the elastic component and the Laplace pressure:

$$P = P_{elastic} + P_{surface} = E\left(\frac{5}{6} - \frac{2}{3\lambda_{eq}} - \frac{1}{6(\lambda_{eq})^4}\right) + \frac{2\gamma}{r\lambda}, \quad [1]$$

where γ is the interfacial energy, *r* is the undeformed radius of the cavity, and λ_{eq} is a factor that accounts for the balance between interfacial energy and elasticity at no applied external pressure (15, 17). This equation is plotted in Fig. 1*E* and shows both that smaller cavities require more pressure to expand due to interfacial tension and that expansion is

unbounded after a critical pressure is reached. This critical pressure approaches *E* for larger voids. Fig. 1*F* shows the critical expansion pressure for a hydrogel where *E* = 10 kPa, a modulus of the same order observed in biological tissues (16, 18, 19), against *r*, showing that the Laplace pressure becomes important below 100 μm.

Ball (20) made several contributions to the understanding of cavitation in the 1980s, including eliminating the need to assume an initial void and extending cavitation theory to compressible elastic solids. In addition, cavitation in solids with different defect shapes, stress states, and materials constitutive relationships has been investigated (21–25). This includes materials with complex plasticity, such as metals (26–28). More recently, cavitation driven by humidity (29, 30) or electric fields (31) has also been studied. A discussion of the unmet needs in modeling cavitation is contained in *Limits of Current Models*.

Dynamics. Dynamic effects in cavitation are often significant (for example, in TBI-related cavitation, where strain rates can reach as high as 10^3 s^{-1} during impact events) (7, 32). The dynamics of inertial cavitation were first considered by Rayleigh (9) in describing the pressure–size relationship for a spherical gas bubble in an infinite liquid medium:

$$P = \rho\left[R\frac{d^2R}{dt^2} + \frac{3}{2}\left(\frac{dR}{dt}\right)^2\right], \quad [2]$$

where ρ is the liquid density, *t* is time, and *R* is the bubble radius. Eq. **2** can be extended to soft solids by adding the elasticity and surface tension terms, which are given in Eq. **1** in *Elasticity and Surface Energy Formulation for Cavitation*.

In addition to inertial effects, viscoelasticity can play an important role at both high and low strain rates. Most soft solids exhibit viscoelastic behavior, and cavitation rheology techniques (see Fig. 3) span strain rates from the quasistatic regime (10^{-4} s^{-1}) to the ultrahigh strain rate regime (10^8 s^{-1}) (33–36). Furthermore, both the strain and strain rate inside a cavitating soft solid can vary dramatically, leading to spatially dependent viscoelastic contributions to cavity dynamics (37–39). A discussion of the unmet
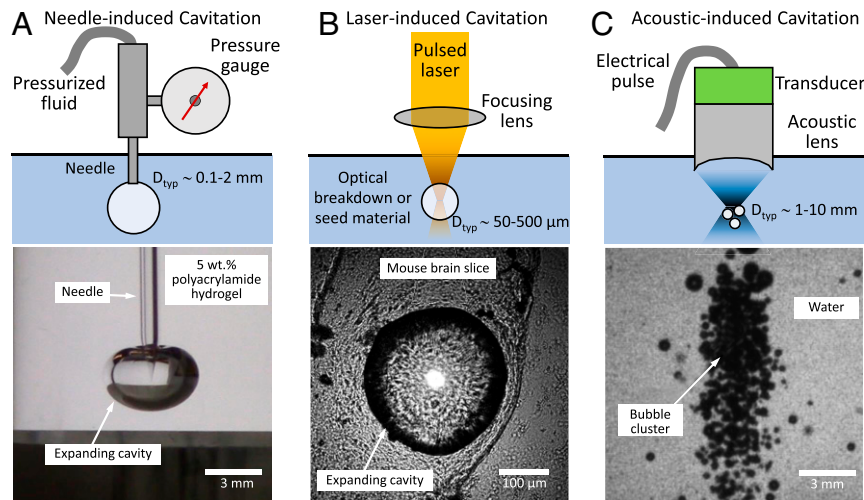
Fig. 2. Schematic and image of cavity formation in (*A*) NIC, (*B*) LIC, and (*C*) AIC. Reprinted by permission from ref. 66 (Copyright 2003, Springer Nature: Doklady Physics).

needs in the dynamics of cavitation is contained in *Experimental Characterization Challenges* and *Needs in Materials Synthesis*.

Cavitation and Fracture. While cavitation in soft solids can be elastic, reversible deformation, voids, or defects in a soft solid can also directly or transitionally expand through fracture (14, 40, 41). Fracture is an inelastic, irreversible process involving the rupture of bonds (42). Although cavitation and fracture are different physical processes, differentiating them and understanding their interrelationship have been challenging (40, 43–46). For soft solids, the question of whether critical deformations are associated with cavitation or fracture is highly relevant for many applications, such as materials characterization (17, 47, 48), design of pressure-sensitive adhesives (42, 49, 50), and understanding damage of biological tissues (3).

Cavitation Rheology Measurements

The term cavitation rheology was introduced in 2007 by Zimberlin et al. (51) to refer to the characterization technique where a pressurized fluid, either gas or liquid, is injected at the tip of a needle embedded in a gel (i.e., needle-induced cavitation [NIC]), and it has since been widely adopted (17, 18, 35, 36, 47, 51–65). As a diverse set of independently developed cavitation-based characterization techniques has emerged, cavitation rheology has grown to encompass a broad set of characterization methods in addition to NIC (Fig. 2) that rely on the rich dynamics, size scales, and positional sensitivities of cavitation to assess materials

properties and behavior. Table 1 contains further information on the dynamic range, spatial sensitivity, and comparison between cavitation rheology and traditional characterization techniques (18, 47, 51, 62, 67).

Goals of Cavitation Rheology. An overarching goal of cavitation rheology is to exploit the underlying physical principles of cavitation to characterize materials. The ranges of size scales and strain rates over which cavitation rheology operates, summarized in Table 1, make it particularly attractive. Many of these techniques are focused toward soft materials and biological tissues, where standard techniques have issues with clamping, slip, and slump. The inherent complexity of biological tissues makes characterizing them the most demanding application of cavitation rheology (18, 55, 68); however, the unique capability of characterizing properties in the body offers significant promise (53, 69).

Also, cavitation rheology is also used to identify, quantify, and potentially control damage due to cavitation events. Cavitation has long been indicated as a damage mechanism in traumatic tissue injury, but exactly how to quantify the amount of short- and long-term damage caused by cavitation remains an open question (70). Controlling cavitation could lead to strategies to mitigate damage from traumatic cavitation-inducing events, such as high impact and blast situations, or to new therapeutic treatments, similar to breaking up kidney stones.

Below, we introduce three broad categories of cavitation rheology methods.

Table 1. Comparison of the dynamic range, spatial sensitivity, and maximum operating pressures for various cavitation rheology and traditional characterization techniques

Technique	Strain rate* (s⁻¹)	Size scale (μm)	Pressure (Pa)	Single cavity
NIC	$10^{-4} - 10^3$	$10^0 - 10^3$	$\leq 10^5$	Yes
LIC	$10^1 - 10^8$	$10^{-1} - 10^2$	$< 10^8$	Yes
AIC	$10^3 - 10^8$	10^3	$\leq 10^7$	No
CIC	$10^{-5} - 10^1$	$10^0 - 10^3$	$\leq 10^7$	No
SIC	$10^{-5} - 10^1$	$10^0 - 10^3$	$\leq 10^7$	No
Shear rheology	$10^{-3} - 10^2$	$10^3 - 10^5$	N/A	N/A
Dynamic uniaxial extension	$10^{-3} - 10^2$	$10^3 - 10^5$	N/A	N/A
Indentation	$10^{-5} - 10^1$	$10^0 - 10^4$	N/A	N/A

*Strain rates were calculated excluding ranges only accessible through time–temperature superposition. N/A, not applicable.

NIC. NIC, as illustrated in Fig. 2*A*, consists of two distinct processes: 1) puncture of a sample with a needle (71) and 2) pressurization of a fluid at the tip of the embedded needle until rapid deformation of the sample occurs at a critical pressure value (51, 67). The small volume of the measurement, r^3, along with the maneuverability of a needle makes NIC a local measurement with strong position control. When deformation is driven by elasticity, a simplified version of Eq. **1** is used to relate the critical pressure P_c to the elastic modulus E of the sample (17, 18, 35, 36, 47, 51–59, 62):

$$P_c = \frac{2\gamma}{r} + \frac{5}{6}E. \qquad [3]$$

While geometric differences in the initial void can cause minor variation (56, 67), more significant variation can be linked to the question of whether the critical pressure is associated with cavitation, fracture, or both. Cavitation and fracture mechanisms, as discussed in *Cavitation and Fracture*, are observed in NIC (47). Critical pressure for fracture initiated expansion P_f in NIC is often modeled with the linear elastic solution for a penny-shaped crack (47, 57, 59–61):

$$P_f = \sqrt{\frac{\pi G_c E}{3r}}. \qquad [4]$$

Hence, if fracture is known or assumed to control the initial deformation, then this equation can be used to characterize G_c, the critical strain energy release rate for fracture. Hutchens et al. (17) have provided a more detailed discussion of the analysis for the different deformation pathways presented above.

The relationships between critical pressure and materials properties that are often used for NIC assume that the samples are well described by a neo-Hookean constitutive relationship. For elastic materials, this assumption has limited influence at the onset of the instability, which often occurs at strains of 30 to 50% (17, 57). As discussed by Pavlovsky et al. (35), viscoelastic effects are also capable of influencing the observed critical pressure. While NIC is typically treated as a quasielastic measurement because the average strain rate on loading is typically of the order 10^{-2} s^{-1}, the pressurization rate can be varied to characterize viscoelastic and poroelastic properties (36).

A significant advantage of NIC is the ability to measure mechanical properties across a broad range of size scales (Table 1). However, this ability complicates measurements when probing size scales similar to that of defects or heterogeneous features in the material. Zhu et al. (72) demonstrated the importance of loading conditions by altering the initial stiffness of the instrument to be either compliant (i.e., fixed pressure conditions) or stiff (i.e., fixed volume) loading conditions. Raayai-Ardakani et al. (48, 62) have recently exploited fixed volume conditions to characterize materials properties before and after the critical event to develop a method well suited for characterizing materials stiffer than those typically tested with pressure-controlled systems.

Laser-Induced Cavitation. Laser-induced cavitation (LIC) (73), as shown in Fig. 2*B*, takes advantage of focused optical energy absorption to cause a dielectric breakdown in a transparent medium (74), giving rise to a rapid cavity expansion. In the conventional approach, a high-intensity optical field, typically achieved using a focused laser pulse, ionizes molecules in a transparent (or dielectric) specimen. As ionization substantially increases optical absorption, an avalanche process driven by positive feedback between ionization and optical absorption leads to an abrupt temperature rise and subsequent cavitation at nanosecond timescales and with high expansion speeds (100 to 3,000 m/s). Due to the sensitivity of the initiation and avalanche processes to local variation of material properties, conventional LIC can be less predictable and difficult to quantify with regard to energetics, especially for heterogeneous media, such as biological tissues.

An alternative approach introduces laser-absorbing particles into the specimen to allow for optical energy absorption without the need for nonlinear dielectric breakdown of the medium (75). In this seeded laser-induced cavitation (SLIC), cavitation is significantly less dependent on the optical properties of the test specimens, and the analysis can be more quantitative.

LIC and SLIC have both been broadly applied for tissue imaging and therapy (76), cell lysis (77), drug delivery (78), microfluidic actuation (79), and dynamic mechanical characterization (39). In Estrada et al. (39), a bubble in a gel first rapidly expands to its maximum size and then, oscillates. By fitting theoretical predictions for the oscillations, the viscoelastic responses were quantified through a generalized Kelvin–Voigt model (39). In the case of biological specimens since optical heterogeneity hinders the propagation of optical waves, an optical fiber can be advantageous for LIC within a thick tissue specimen (80, 81). Due to the typical timescale of the cavitation dynamics, which ranges from milliseconds to microseconds, the real-time observation of LIC process is usually achieved by high-frame rate cameras (39). As demonstrated in Fig. 2, fast-repetition rate illumination sources, such as a femtosecond oscillator with a pulse picking system, can be employed in a complementary manner for ultrafast stroboscopic imaging of LIC or SLIC.

Acoustic-Induced Cavitation. Acoustic-induced cavitation (AIC), as shown in Fig. 2*C*, typically occurs when rapid cycles of large positive and negative pressure are created by high-frequency (kilohertz to megahertz) mechanical vibration. The intense mechanical vibration is achieved either through a direct contact with an ultrasonic transducer or through focused acoustic waves transmitted through a testing medium. AIC using electric transducers has been widely applied to various processes for food (82), energy (83), and nanomaterials (84). Moreover, AIC has long been used in diagnostic and therapeutic applications. For example, focused acoustic energy can alter tissue permeability in cancer treatment, enhancing drug performance and gene delivery (85). In these medical applications, AIC plays a significant role since oscillating and collapsing cavities enhance cellular gene delivery and extravasation. High-intensity focused ultrasound has been applied for destructive applications, such as surgery of premetastatic cancers and lithotripsy, where controlled cavitation can improve the speed and efficacy of the treatments.

Despite the extensive applications of AIC, the rheological applications of AIC are relatively unexplored. In contrast to NIC and LIC, AIC produces a cavitation cloud consisting of microbubbles; thus, collective characteristics of AIC, such as a threshold of the cloud cavitation (86), are preferentially introduced instead of the cavity dynamics of a single bubble.

Other Cavitation Methods. The techniques discussed in this section are other common examples of cavitation; however, they lack the dynamic and positional control often sought for controlled studies. **Shockwave-induced cavitation.** The direct dynamic effect of shockwaves on interfaces (i.e., cavitation) can be observed in certain media, such as water and tissues on occasion. Cavitation bubbles

occur after the pressure/tension alternating load of a shockwave passes the medium (e.g., heart valve cavitation in Fig. 1*C*) (1). Many bubbles grow and then, violently collapse while emitting secondary spherical shockwaves. As the shockwave scatters from the proximal cloud surface, a new section of the cloud is generated with each cycle. Shockwave-induced cavitation (SIC), a broad subsection that includes AIC, techniques include drop tower (41), Split–Hopkinson or Kolsky bar (4, 8), and controlled blast (87) setups.

Confinement-induced cavitation. Controlled cavitation events can also occur in specimen geometries where material incompressibility and confining boundaries lead to large hydrostatic pressures in response to a far-field mechanical stress (e.g., knuckle cracking in Fig. 1*B*) (2). The most common method for controlling such confinement-induced cavitation (CIC) events is uniaxially loading a short cylindrical disc rigidly bonded between two plates (14, 88–90). This geometry provided the first evidence of cavitation in soft solids (12–14).

Challenges and Unmet Needs

Limits of Current Models. **Current discrepancies.** While significant progress has been made in developing cavitation techniques as characterization methods, challenges remain in modeling observed experimental phenomena. Postinstability modeling of cavitation is still limited in both NIC and LIC. In NIC, current experimental protocols exploit the onset of the instability to characterize the mechanical properties (17, 47, 51), which are associated with low strain rates. However, primary damage is most likely incurred during the large-strain, high-strain rate expansion stage. While some work has determined the stabilizing stretch of a cavitation event, addressing damage accumulation during expansion is nontrivial due to the complex large-strain properties of gels and biological tissues (17, 19, 57, 72). In LIC, expansion dynamics have been largely untreated, and the postexpansion modeling has been on inertial effects and viscoelastic dissipation (39). Fracture processes in LIC have been untreated and unexplored.

Local structure and cavity nucleation. Modeling cavitation in both solids and fluids is often based on continuum mechanics. However, continuum-level models probe size scales much larger than molecular size scales, and continuum models of cavitation growth assume an initial seeded void site with a specified size. Whether this defect in real materials is an impurity in the sample or a local region of the network where the modulus varies significantly from the bulk remains insufficiently understood. In addition, it is challenging to obtain insights into the transition from cavity expansion to crack initiation and propagation using continuum mechanics models. Recent efforts in glasses, another class of disordered solids, have shown that the response and failure of the material are heavily dictated by the local packing (91) and that certain regions in the sample are more prone to failure than others (92, 93). A similar question can be posed for disordered soft materials, such as polymer networks: is the local network structure important in determining the initial formation and growth of cavity sites, and what must the size of the cavity be before continuum mechanics results can be accurately applied? Is the mesh size of the network the characteristic length that must be exceeded, or is the elastocapillary length the appropriate scale? Molecular dynamics (MD) simulations are expected to play an important role in addressing these issues and connecting to continuum mechanics model length scales, but given the noisy nature of stress data calculated from MD, large-scale simulations with explicit solvent will likely be required to bridge these length scales.

Experimental Characterization Challenges. **Bridging experimental timescales.** Cavitation rheology techniques span a large range of strain rates and moduli. A summary plot of strain rate against shear moduli measured with different cavitation rheology techniques taken from literature is shown in Fig. 3 with bands representing strain rates during common impact loadings. Considering the data in Fig. 3, one can see that there are still gaps in the current capabilities of cavitation rheology. Comparing the NIC and LIC envelopes, one can see that these characterization techniques operate in distinct regimes, with LIC being a high-strain rate technique and NIC occupying the low-strain regime. Importantly, there are at least two decades separating the properties extracted from each technique. Expanding the capabilities of either technique to bridge this gap is a subject of future interest. Decreasing the pressurization time of NIC to increase strain rate seems to be a viable experimental protocol to accomplish this goal (105).

Distinguishing cavitation from fracture. Experimentally distinguishing cavitation and fracture mechanisms is a significant challenge in cavitation rheology. Gent and Wang (43) first considered this challenge to a limited degree. However, interest in this transition between cavitation and fracture was renewed when Kundu and Crosby (47) experimentally demonstrated that softer solids exhibit a transition from fracture to cavitation at smaller size scales. Following this work, Hutchens et al. (17) used existing theory to generate phase maps of the cavitation and fracture regimes (44, 72). The transition between the two mechanisms was complicated by the fracture criterion often being met during the cavitation expansion. Raayai-Ardakani et al. (48) recently suggested that expansion is not driven solely by fracture and is simultaneously driven by both cavitation and fracture. However, they seem to broadly define cavitation as including any elastic stretching that occurs during the fracture process, whereas cavitation does not occur unless the threshold cavitation pressure is realized.
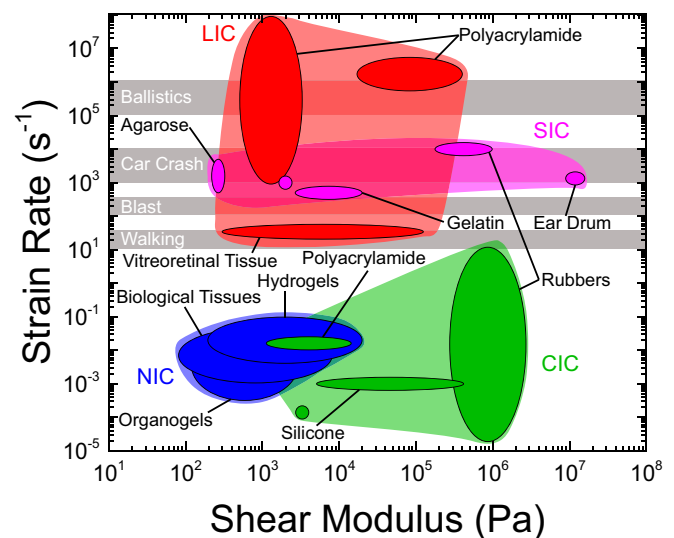

Fig. 3. Plot of strain rate against shear modulus for NIC, LIC, SIC, and CIC values from the literature. AIC was omitted from the plot due to difficulties in estimating a strain rate for measurements. NIC strain rates were taken as those associated with the properties extracted from the measurement and are thus much lower than values associated with the expansion stage. Bands for strain rates of common blast or impact activities are overlaid on the data (4, 8, 14, 17, 18, 35, 36, 39, 47, 49, 51, 52, 55, 57, 58, 60, 61, 68, 87, 88, 90, 94–104).

Observing the void morphology after expansion is insufficient for determining whether or not the deformation was initiated by a fracture process (17). Visualization of the void during the early expansion stage could resolve this ambiguity in the extremes where purely elastic cavitation forms a smooth, spherical bubble and simple crack propagation forms a rough, planar surface. However, soft solids have been found to be particularly susceptible to elastic crack blunting, which could make a fracture process look like a cavitation process in the early stages of expansion (106). Blunting may present itself in NIC, where pressures approach E, but should be dynamically present in LIC, where the sample is subjected to pressures well above E over a nanosecond timescale. Another solution for NIC is to vary the radius of the needle and observe the size-scale dependence of the critical pressure. As shown in Eqs. **3** and **4**, cavitation should have a linear dependence on $1/r$, while fracture should scale with $1/\sqrt{r}$ (47). This solution is limited in that it requires multiple measurements and may not be applicable to small-volume biological samples.

Visualization during and after cavitation. One of the main challenges associated with cavitation is the validation and visualization of a cavitation event, particularly in vivo. Synthetic models are often chosen for transparency, but visualizing a cavitation event is difficult to impossible in opaque tissues. The most common methods of analysis are postdamage MRI and fixing and staining tissue for histopathological analyses. Another method is diffusion tensor imaging, which is sensitive to axonal injury (107). Additionally, there are methods that combine multiple tools (ultrasound, computed tomography scan, and MRI) to analyze cavitation effects for the purpose of developing two-dimensional and three-dimensional (3D) finite difference time domain simulations (108). Thus far, there are no methods that have the capability to detect small-scale cavitation damage on intact tissue in real time. One possibility could be to use NIC or LIC on tissues and image cavitation in real time. Although there have been no successful attempts at visualizing a single bubble cavitation on a fully intact tissue, it is possible to visualize a single bubble cavitation on a thin slice of brain and determine resulting damage to the tissue (8). LIC can be performed on a slice of tissue that is thin enough to be transparent; however, the slicing process alters the 3D integrity of the tissue. To visualize cavitation on a whole intact tissue, one must clarify the tissue. There are two approaches to clearing tissues, solvent-based methods and aqueous methods (109). Although solvent-based methods effectively clear the tissue, the process alters the structure of the tissue by dehydration and lipid removal, making the results inapplicable to real tissue environments. Currently, the best option for visualizing a cavitation event is to fix and stain the tissue immediately after cavitation, allowing for postdamage analysis, similar to the majority of histological analyses performed on animal models undergoing head trauma experiments (110). The ability to visualize a cavitation event in real time is a significant unmet need in the field.

Needs in Materials Synthesis. Cavitation and chemistry. Since the field of cavitation rheology is in its infancy, only a few synthetic systems have been characterized. Gent and coworkers (43, 88) performed many experiments on rubbers. In solvent swollen systems, studies have been performed on physically cross-linked gels, such as agarose and amphiphilic block copolymers (51, 111) and self-assembled organogels (60, 61), and on covalently linked networks, such as polyacrylamide (PAAm) gels (39, 47, 51, 112). However, these systems are "off-the-shelf" materials chosen for convenience rather than specifically designed systems. The

development of new materials could drive improved understanding of cavitation in soft materials. The rapid expansion of synthetic chemistry has provided elastic networks with improved connectivity and homogeneity. For example, photo-initiated thiolene chemistry generated bio-inspired networks with excellent resiliency (113).

Cavitation rheology has started to provide a different understanding for some well-studied systems. For example, the mechanical properties of PAAm networks are well established by classical methods in the literature. Although PAAm gels (E = 30 kPa) have high resilience at low strains, they are known to be brittle with a strain at break of 40%. More recently, however, high extension values, roughly 300%, in PAAm gels (G = 3 to 10 kPa) were achieved using inertial microcavitation high-strain rate rheometry (39). This discrepancy shows that cavitation phenomenon will provide a different perspective to the field, which classical mechanical testing methods cannot provide.

Another important tool in understanding the stress profile in a cavitation event could be the emergence of so-called "mechanochemistry." Mechanochromism, a subsection of mechanochemistry, produces color change with mechanical force and is inspired by natural phenomena, such as sonoluminescence (114). In this field, spiropyran-based materials have received significant attention with their ability to turn into a colored merocyanine form in response to applied stress (115, 116).

Dynamic systems. Biological materials are rich in hydrogen bonds, agarose is gelled with calcium, and titan is known to unfold in multiple steps as the tertiary structure of the protein unravels (117, 118). The continued advancement of highly functionalized, elastic materials is expected to inform cavitation. Beyond improvements in network connectivity and multicomponent systems, the inclusion of dynamic interactions seems to be a rich field ripe for exploration (119–121). In addition to tailored hydrogen bonding units, metal–ligand interactions that provide tunable interaction strengths and lifetime have been studied (122–124). The inclusion
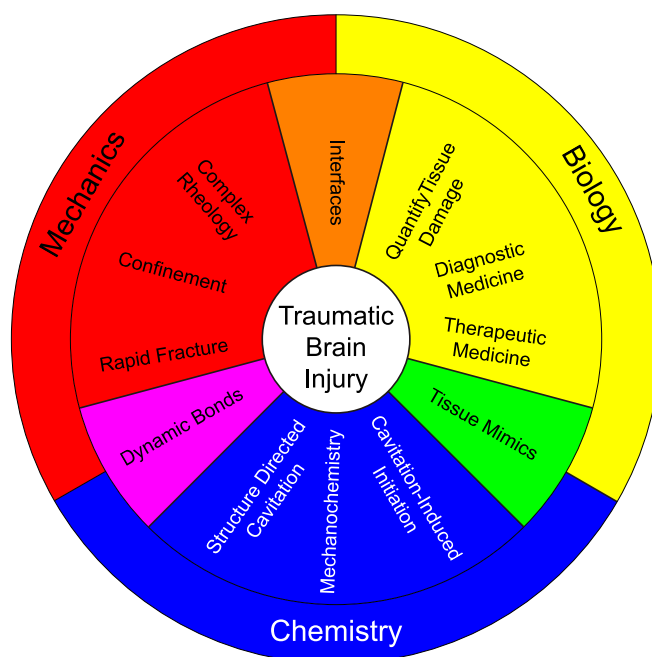

Fig. 4. Graphic representation of exclusive and overlapping opportunities for further research in the mechanics, biology, and chemistry communities.

of folding domains should add new complexity to the cavitation behavior and enable networks to better mimic complex tissues.

Emerging Opportunities

The concepts involved in motivating and addressing the needs and challenges in *Challenges and Unmet Needs*, schematically summarized in Fig. 4, are highly interdisciplinary and vary in scope from applied to deeply fundamental questions that will impact fields beyond cavitation. The versatility in controlling and characterizing complex material response and structure at different size scales and strain rates uniquely qualifies cavitation rheology to address those questions with broader impact. The following subsections summarize open questions discussed fully in *Challenges and Unmet Needs*, where different communities have the opportunity to contribute to the field of cavitation.

Mechanics and Physics. Cavitation rheology is poised to benefit from multiple developments across the mechanics and physics communities. There are currently multiple technical challenges in both the modeling and analysis of cavitation experiments. These challenges lead us to the following open questions.

- How do cavitation deformations change in confined systems or near phase interfaces?
- How can cavitation be distinguished from fracture?
- What structural size scales dominate for the nucleation and growth of cavities?
- Can current techniques be improved or new techniques created to bridge the experimental gaps in timescale?

Biology. From applications in tissue characterization to therapeutic and diagnostic medicine, cavitation rheology has immense potential in the field of biology. With regard to injury, specifically TBI, this technique can be utilized to induce cavitation at specific locations within the brain to not only quantify local modulus but also, connect how those variations in moduli correlate with remote tissue and cellular cavitation damage potentially leading to mild TBI. By engaging these questions, biologists will satisfy the overarching goal of establishing cavitation rheology as a foundational tool for characterizing the mechanical response of soft biological tissues.

- How can cavitation rheology be adapted to improve the measurement of confined in vivo tissue mechanical properties?

- What methods enable cavitation dynamics in opaque tissues to be visualized and quantified?
- How is tissue damage from cavitation events best detected and quantified?
- What therapeutic treatments can cavitation enable or enhance?

Chemistry. While the world of cavitation seems to be historically the realm of engineers and physicists, there are growing opportunities for synthetic chemistry to contribute to the field. The chemistry community will significantly aid both the mechanics and biology communities in understanding the physical principles of cavitation as well as using them to advantage in chemical reactions.

- How can new materials, such as mechanophores, be used to simplify challenges in cavitation characterization?
- Can relaxation timescales of a network dictate expansion and collapse behavior in a cavitation event?
- Can damage due to cavitation be directed or mitigated through structural control of materials?
- How can cavitation be used to enable spatially controlled initiation in chemical reactions?

Conclusions

Cavitation rheology is a broad field coalescing from the development of characterization, diagnostic, and therapeutic techniques that exploit the underlying physics of cavitation. Cavitation rheology uniquely offers the ability to tune size scales and strain rates from the macro- to microscales and from low to high strain rates, respectively. The larger unmet needs and challenges of cavitation rheology offer opportunities for researchers to contribute toward expanding our knowledge of how soft materials, especially soft tissues, absorb deformation and develop irreversible damage.

Data Availability

No direct data were used in creating the content of this perspective.

1 E. Rambod, M. Beizaie, M. Shusser, S. Milo, M. Gharib, A physical model describing the mechanism for formation of gas microbubbles in patients with mitral mechanical heart valves. *Ann. Biomed. Eng.* **27**, 774–792 (1999).
2 G. N. Kawchuk, J. Fryer, J. L. Jaremko, H. Zeng, Real-time visualization of joint cavitation. *PLoS One* **10**, 1–11 (2015).
3 Y. Kurosawa *et al.*, Basic study of brain injury mechanism caused by cavitation. *Conf. Proc. IEEE Eng. Med. Biol. Soc.* **2009**, 7224–7227 (2009).
4 Y. Hong, M. Sarntinoranont, G. Subhash, S. Canchi, M. A. King, Localized tissue surrogate deformation due to controlled single bubble cavitation. *Exp. Mech.* **56**, 97–109 (2016).
5 R. Salzar, D. Treichler, A. Wardlaw, G. Weiss, J. Goeller, Experimental investigation of cavitation as a possible damage mechanism in blast-induced traumatic brain injury in post-mortem human subject heads. *J. Neurotrauma* **34**, 1589–1602 (2017).
6 U. Adhikari, A. Goliaei, M. Berkowitz, Nanobubbles, cavitation, shock waves and traumatic brain injury. *Phys. Chem. Chem. Phys.* **18**, 32638–32652 (2016).
7 J. Goeller, A. Wardlaw, D. Treichler, J. O'Bruba, G. Weiss, Investigation of cavitation as a possible damage mechanism in blast-induced traumatic brain injury. *J. Neurotrauma* **29**, 1589–1602 (2012).
8 S. Canchi *et al.*, Controlled single bubble cavitation collapse results in jet-induced injury in brain tissue. *J. Mech. Behav. Biomed. Mater.* **74**, 261–273 (2017).
9 L. Rayleigh, On the pressure developed in a liquid during the collapse of a spherical cavity. *London Edinburgh Dublin Philos. Mag. J. Sci.* **34**, 94–98 (1917).
10 F. P. Bundy, H. T. Hall, H. M. Strong, R. H. Wentorf, Man-made diamonds. *Nature* **176**, 51–55 (1955).
11 P. Johansen, Mechanical heart valve cavitation. *Expet Rev. Med. Dev.* **1**, 95–104 (2004).
12 W. F. Busse, Physics of rubber as related to the automobile. *J. Appl. Phys.* **9**, 438–451 (1938).
13 F. L. Yerzley, Adhesion of neoprene to metal. *Ind. Eng. Chem.* **31**, 950–956 (1939).
14 A. N. Gent, P. Lindley, Internal rupture of bonded rubber cylinders in tension. *Proc. R. Soc. London Ser. A* **249**, 195–205 (1959).

15 A. N. Gent, D. A. Tompkins, Surface energy effects for small holes or particles in elastomers. *Rubber Chem. Technol.* **43**, 873–877 (1970).

16 B. Ahn, J. Kim, Measurement and characterization of soft tissue behavior with surface deformation and force response under large deformations. *Med. Image Anal.* **14**, 138–148 (2010).

17 S. B. Hutchens, S. Fakhouri, A. J. Crosby, Elastic cavitation and fracture via injection. *Soft Matter* **12**, 2557–2566 (2016).

18 L. E. Jansen, N. P. Birch, J. D. Schiffman, A. J. Crosby, S. R. Peyton, Mechanics of intact bone marrow. *J. Mech. Behav. Biomed. Mater.* **50**, 299–307 (2015).

19 G. A. Holzapfel, R. W. Ogden, Constitutive modelling of arteries. *Proc. Math. Phys. Eng. Sci.* **466**, 1551–1597 (2010).

20 J. Ball, Discontinuous equilibrium solutions and cavitation in nonlinear elasticity. *Philos. Trans. R. Soc. A* **306**, 557–611 (1982).

21 J. Sivaloganathan, S. J. Spector, A construction of infinitely many singular weak solutions to the equations of nonlinear elasticity. *Proc. R. Soc. Edinburgh Sect. A Math. Phys. Sci.* **132**, 985–992 (2002).

22 J. Sivaloganathan, S. J. Spector, V. Tilakraj, The convergence of regularized minimizers for cavitation problems in nonlinear. *SIAM J. Appl. Math.* **66**, 736–757 (2006).

23 O. Lopez-Pamies, M. I. Idiart, T. Nakamura, Cavitation in elastomeric solids. I. A defect-growth theory. *J. Mech. Phys. Solid.* **59**, 1464–1487 (2011).

24 T. Nakamura, O. Lopez-Pamies, A finite element approach to study cavitation instabilities in non-linear elastic solids under general loading conditions. *Int. J. Non Lin. Mech.* **47**, 331–340 (2012).

25 O. Lopez-Pamies, Onset of cavitation in compressible, isotropic, hyperelastic solids. *J. Elasticity* **94**, 115–145 (2009).

26 T. Pardoen, J. W. Hutchinson, Extended model for void growth and coalescence. *J. Mech. Phys. Solid.* **48**, 2467–2512 (2000).

27 J. W. Hutchinson, Constitutive behavior and crack tip fields for materials undergoing creep-constrained grain boundary cavitation. *Acta Metall.* **31**, 1079–1088 (1983).

28 Y. Huang, J. W. Hutchinson, V. Tvergaard, Cavitation instabilities in elastic-plastic solids. *J. Mech. Phys. Solids* **39**, 223–241 (1991).

29 H. Wang, S. Cai, Drying-induced cavitation in a constrained hydrogel. *Soft Matter* **11**, 1058–1061 (2015).

30 H. Wang, S. Cai, Cavitation in a swollen elastomer constrained by a non-swellable shell. *J. Appl. Phys.* **117**, 154901 (2015).

31 Q. Wang, Z. Suo, X. Zhao, Bursting drops in solid dielectrics caused by high voltages. *Nat. Commun.* **3**, 1157 (2012).

32 M. Sarntinoranont et al., High-strain-rate brain injury model using submerged acute rat brain tissue slices. *J. Neurotrauma* **29**, 418–429 (2012).

33 L. Mancia, E. Vlaisavljevich, Z. Xu, E. Johnsen, Predicting tissue susceptibility to mechanical cavitation damage in therapeutic ultrasound. *Ultrasound Med. Biol.* **43**, 1421–1440 (2017).

34 E. Bar-Kochba, M. T. Scimone, J. B. Estrada, C. Franck, Strain and rate-dependent neuronal injury in a 3D in vitro compression model of traumatic brain injury. *Sci. Rep.* **6**, 1–11 (2016).

35 L. Pavlovsky, M. Ganesan, J. G. Younger, M. J. Solomon, Elasticity of microscale volumes of viscoelastic soft matter by cavitation rheometry. *Appl. Phys. Lett.* **105**, 1–5 (2014).

36 A. Delbos, J. Cui, S. Fakhouri, A. J. Crosby, Cavity growth in a triblock copolymer polymer gel. *Soft Matter* **8**, 8204 (2012).

37 A. Kumar, D. Aranda-Iglesias, O. Lopez-Pamies, Some remarks on the effects of inertia and viscous dissipation in the onset of cavitation in rubber. *J. Elasticity* **126**, 201–213 (2017).

38 R. Gaudron, M. T. Warnez, E. Johnsen, Bubble dynamics in a viscoelastic medium with nonlinear elasticity. *J. Fluid Mech.* **766**, 54–75 (2015).

39 J. B. Estrada, C. Barajas, D. L. Henann, E. Johnsen, C. Franck, High strain-rate soft material characterization via inertial cavitation. *J. Mech. Phys. Solid.* **112**, 291–317 (2018).

40 M. L. Williams, R. A. Schapery, Spherical flaw instability in hydrostatic tension. *Int. J. Fract. Mech.* **1**, 64–72 (1965).

41 J. Kang, C. Wang, S. Cai, Cavitation to fracture transition in a soft solid. *Soft Matter* **13**, 6372–6376 (2017).

42 C. Creton, M. Ciccotti, Fracture and adhesion of soft materials: A review. *Rep. Prog. Phys.* **79**, 046601 (2016).

43 A. N. Gent, C. Wang, Fracture mechanics and cavitation in rubber-like solids. *J. Mater. Sci.* **26**, 3392–3395 (1991).

44 J. Diani, Irreversible growth of a spherical cavity in rubber-like material: A fracture mechanics description. *Int. J. Fract.* **112**, 151–161 (2001).

45 Y. Y. Lin, C. Y. Hui, Cavity growth from crack-like defects in soft materials. *Int. J. Fract.* **126**, 205–221 (2004).

46 L. A. Archer, D. Ternet, R. G. Larson, "Fracture" phenomena in shearing flow of viscous liquids. *Rheol. Acta* **36**, 579–584 (1997).

47 S. Kundu, A. J. Crosby, Cavitation and fracture behavior of polyacrylamide hydrogels. *Soft Matter* **5**, 3963 (2009).

48 S. Raayai-Ardakani, D. R. Earl, T. Cohen, The intimate relationship between cavitation and fracture. *Soft Matter* **15**, 4999–5005 (2019).

49 A. J. Crosby, K. R. Shull, H. Lakrout, C. Creton, Deformation and failure modes of adhesively bonded elastic layers. *J. Appl. Phys.* **88**, 2956–2966 (2000).

50 H. Lakrout, P. Sergot, C. Creton, Direct observation of cavitation and fibrillation in a probe tack experiment on model acrylic pressure-sensitive-adhesives. *J. Adhes.* **69**, 307–359 (1999).

51 J. A. Zimberlin, N. Sanabria-DeLong, G. N. Tew, A. J. Crosby, Cavitation rheology for soft materials. *Soft Matter* **3**, 763 (2007).

52 J. A. Zimberlin, A. J. Crosby, Water cavitation of hydrogels. *J. Polym. Sci. B Polym. Phys.* **45**, 1423–1427 (2010).

53 J. A. Zimberlin, J. J. McManus, A. J. Crosby, Cavitation rheology of the vitreous: Mechanical properties of biological tissue. *Soft Matter* **6**, 3632 (2010).

54 Y. Liu, A. Lloyd, G. Guzman, K. A. Cavicchi, Polyelectrolyte-surfactant complexes as thermoreversible organogelators. *Macromolecules* **44**, 8622–8630 (2011).

55 J. Cui, C. H. Lee, A. Delbos, J. J. McManus, A. J. Crosby, Cavitation rheology of the eye lens. *Soft Matter* **7**, 7827 (2011).

56 S. B. Hutchens, A. J. Crosby, Soft-solid deformation mechanics at the tip of an embedded needle. *Soft Matter* **10**, 3679–3684 (2014).

57 S. M. Hashemnejad, S. Kundu, SI: Nonlinear elasticity and cavitation of a triblock copolymer gel. *Soft Matter* **11**, 4315–4325 (2015).

58 K. C. Bentz, S. E. Walley, D. A. Savin, Solvent effects on modulus of poly(propylene oxide)-based organogels as measured by cavitation rheology. *Soft Matter* **12**, 4991–5001 (2016).

59 B. R. Frieberg et al., Viscoplastic fracture transition of a biopolymer gel. *Soft Matter* **14**, 4696–4701 (2018).

60 P. Fei, S. J. Wood, Y. Chen, K. A. Cavicchi, Maximum bubble pressure rheology of low molecular mass organogels. *Langmuir* **31**, 492–498 (2015).

61 S. M. Hashemnejad, M. M. Huda, N. Rai, S. Kundu, Molecular insights into gelation of di-fmoc-L-lysine in organic solvent–water mixtures. *ACS Omega* **2**, 1864–1874 (2017).

62 S. Raayai-Ardakani, Z. Chen, D. Earl, T. Cohen, Volume-controlled cavity expansion for probing of local elastic properties in soft materials. *Soft Matter* **15**, 381–392 (2018).

63 S. M. Hashemnejad, S. Kundu, Rheological properties and failure of alginate hydrogels with ionic and covalent crosslinks. *Soft Matter* **15**, 7852–7862 (2019).

64 K. C. Bentz, N. Sultan, D. A. Savin, Quantitative relationship between cavitation and shear rheology. *Soft Matter* **14**, 8395–8400 (2018).

65 A. M. Fuentes-Caparros, B. Dietrich, L. Thomson, C. Chauveau, D. Adams, Using cavitation rheology to understand dipeptide-based low molecular weight gels. *Soft Matter* **15**, 6340–6347 (2019).

66 G. N. Sankin, V. S. Teslenko, Two-threshold cavitation regime. *Dokl. Phys.* **48**, 665–668 (2003).

67 C. W. Barney, Y. Zheng, S. Wu, S. Cai, A. J. Crosby, Residual strain effects in needle-induced cavitation. *Soft Matter* **15**, 7390–7397 (2019).

68 S. Polio et al., Cross-platform mechanical characterization of lung tissue. *PLoS One* **13**, 1–17 (2018).

69 A. Manduca et al., Magnetic resonance elastography: Non-invasive mapping of tissue elasticity. *Med. Image Anal.* **5**, 237–254 (2001).

70 P. A. Taylor, J. S. Ludwigsen, C. C. Ford, Investigation of blast-induced traumatic brain injury. *Brain Inj.* **28**, 879–895 (2014).

71 S. Fakhouri, S. B. Hutchens, A. J. Crosby, Puncture mechanics of soft solids. *Soft Matter* **11**, 4723–4730 (2015).

72 J. Zhu, T. Li, S. Cai, Z. Suo, Snap-through expansion of a gas bubble in an elastomer. *J. Adhes.* **87**, 466–481 (2011).

73 C. S. Peel, X. Fang, S. R. Ahmad, Dynamics of laser-induced cavitation in liquid. *Appl. Phys. A* **103**, 1131–1138 (2011).

74 C. A. Sacchi, Laser-induced electric breakdown in water. *J. Opt. Soc. Am. B* **8**, 337 (1991).

75 Y. Arita, M. Antkowiak, V. Venugopalan, F. J. Gunn-Moore, K. Dholakia, Dynamics of primary and secondary microbubbles created by laser-induced breakdown of an optically trapped nanoparticle. *Phys. Rev. E* **85**, 016319 (2012).

76 Cw. Wei *et al.*, Laser-induced cavitation in nanoemulsion with gold nanospheres for blood clot disruption: In vitro results. *Opt. Lett.* **39**, 2599 (2014).

77 K. R. Rau, P. A. Quinto-Su, A. N. Hellman, V. Venugopalan, Pulsed laser microbeam-induced cell lysis: Time-resolved imaging and analysis of hydrodynamic effects. *Biophys. J.* **91**, 317–329 (2006).

78 T. H. Han, J. J. Yoh, A laser based reusable microjet injector for transdermal drug delivery. *J. Appl. Phys.* **107**, 103110 (2010).

79 K. Zhang *et al.*, Laser-induced thermal bubbles for microfluidic applications. *Lab Chip* **11**, 1389–1395 (2011).

80 M. Mohammadzadeh, S. R. Gonzalez-Avila, K. Liu, Q. J. Wang, C. D. Ohl, Synthetic jet generation by high-frequency cavitation. *J. Fluid Mech.* **823**, 1–12 (2017).

81 R. J. Colchester *et al.*, Laser-generated ultrasound with optical fibres using functionalised carbon nanotube composite coatings. *Appl. Phys. Lett.* **104**, 173502 (2014).

82 W. Wang *et al.*, Acoustic cavitation assisted extraction of pectin from waste grapefruit peels: A green two-stage approach and its general mechanism. *Food Res. Int.* **102**, 101–110 (2017).

83 M. J. Madison *et al.*, Mechanical pretreatment of biomass. Part I. Acoustic and hydrodynamic cavitation. *Biomass Bioenergy* **98**, 135–141 (2017).

84 R. Rana, Y. Mastai, A. Gedanken, Acoustic cavitation leading to the morphosynthesis of mesoporous silica vesicles. *Adv. Mater.* **14**, 1414–1418 (2002).

85 E. P. Stride, C. C. Coussios, Cavitation and contrast: The use of bubbles in ultrasound imaging and therapy. *Proc. IME H J. Eng. Med.* **224**, 171–191 (2010).

86 M. Lafond, A. Watanabe, S. Yoshizawa, S. I. Umemura, K. Tachibana, Cavitation-threshold determination and rheological-parameters estimation of albumin-stabilized nanobubbles. *Sci. Rep.* **8**, 7472 (2018).

87 H. Luo, S. Jiang, D. U. Nakmali, R. Z. Gan, H. Lu, Mechanical properties of a human eardrum at high strain rates after exposure to blast waves. *J. Dyn. Behav. Mater.* **2**, 59–73 (2015).

88 K. Cho, A. N. Gent, P. S. Lam, Internal fracture in an elastomer containing a rigid inclusion. *J. Mater. Sci.* **22**, 2899–2905 (1987).

89 V. Lefèvre, K. Ravi-Chandar, O. Lopez-Pamies, Cavitation in rubber: An elastic instability or a fracture phenomenon?. *Int. J. Fract.* **192**, 1–23 (2015).

90 S. Lin, Y. Mao, R. Radovitzky, X. Zhao, Instabilities in confined elastic layers under tension: Fringe, fingering and cavitation. *J. Mech. Phys. Solid.* **106**, 229–256 (2017).

91 E. D. Cubuk *et al.*, Structure-property relationships from universal signatures of plasticity in disordered solids. *Science* **358**, 1033–1037 (2017).

92 A. Shavit, R. A. Riggleman, Strain localization in glassy polymers under cylindrical confinement. *Phys. Chem. Chem. Phys.* **16**, 10301–10309 (2014).

93 R. J. S. Ivancic, R. A. Riggleman, Identifying structural signatures of shear banding in model polymer nanopillars. *Soft Matter* **15**, 4548–4561 (2019).

94 W. Kang, A. Ashfaq, T. O'Shaughnessy, A. Bagchi, Cavitation nucleation in gelatin: Experiment and mechanism. *Acta Biomater.* **67**, 295–306 (2017).

95 S. M. Atay, C. D. Kroenke, A. Sabet, P. V. Bayly, Measurement of the dynamic shear modulus of mouse brain tissue in vivo by magnetic resonance elastography. *J. Biomech. Eng.* **130**, 021013 (2008).

96 G. S. Wilde, H. J. Burd, S. J. Judge, Shear modulus data for the human lens determined from a spinning lens test. *Exp. Eye Res.* **97**, 36–48 (2012).

97 D. Palanker, I. Turovets, A. Lewis, Dynamics of ArF excimer laser-induced cavitation bubbles in gel surrounded by a liquid medium. *Laser Surg. Med.* **21**, 294–300 (1997).

98 S. Canchi *et al.*, Simulated blast overpressure induces specific astrocyte injury in an ex vivo brain slice model. *PLoS One* **12**, e0175396 (2017).

99 Y. Cao *et al.*, Cellular high-energy cavitation trauma—description of a novel in vitro trauma model in three different cell types. *Front. Neurol.* **7**, 10 (2016).

100 B. Arnal, J. Baranger, C. Demene, M. Tanter, M. Pernot, In vivo real-time cavitation imaging in moving organs. *Phys. Med. Biol.* **62**, 843–857 (2017).

101 J. Gateau *et al.*, In vivo bubble nucleation probability in sheep brain tissue. *Phys. Med. Biol.* **56**, 7001–7015 (2011).

102 E. A. Brujan, A. Vogel, Stress wave emission and cavitation bubble dynamics by nanosecond optical breakdown in a tissue phantom. *J. Fluid Mech.* **558**, 281–308 (2006).

103 N. Belayachi, N. Benseddiq, M. Naït-Abdelaziz, A. Hamdi, On cavitation and macroscopic behaviour of amorphous polymer-rubber blends. *Sci. Technol. Adv. Mater.* **9**, 025008 (2008).

104 X. Poulain, V. Lefèvre, O. Lopez-Pamies, K. Ravi-Chandar, Damage in elastomers: Nucleation and growth of cavities, micro-cracks, and macro-cracks. *Int. J. Fract.* **205**, 1–21 (2017).

105 M. P. Milner, S. B. Hutchens, A device to fracture soft solids at high speeds. *Extreme Mech. Lett.* **28**, 69–75 (2019).

106 C. Y. Hui, A. Jagota, S. J. Bennison, J. D. Londono, Crack blunting and the strength of soft elastic solids. *Proc. R. Soc. London, Ser. A* **459**, 1489–1516 (2003).

107 C. L. MacDonald *et al.*, Detection of blast-related traumatic brain injury in U.S. Military personnel. *N. Engl. J. Med.* **364**, 2091–2100 (2011).

108 C. D. Arvanitis, G. T. Clement, N. McDannold, Transcranial assessment and visualization of acoustic cavitation: Modeling and experimental validation. *IEEE Trans. Med. Imag.* **34**, 1270–1281 (2015).

109 D. S. Richardson, J. W. Lichtman, Clarifying tissue clearing. *Cell* **162**, 246–257 (2015).

110 I. Cernak, Animal models of head trauma. *NeuroRX* **2**, 410–422 (2005).

111 J. J. Macoskey *et al.*, Using the cavitation collapse time to indicate the extent of histotripsy-induced tissue fractionation. *Phys. Med. Biol.* **63**, 055013 (2018).

112 J. Tang, J. Li, J. J. Vlassak, Z. Suo, Fatigue fracture of hydrogels. *Extreme Mech. Lett.* **10**, 24–31 (2017).

113 J. Cui, M. A. Lackey, G. N. Tew, A. J. Crosby, Mechanical properties of end-linked PEG/PDMS hydrogels. *Macromolecules* **45**, 6104–6110 (2012).

114 G. Kim *et al.*, High-intensity focused ultrasound-induced mechanochemical transduction in synthetic elastomers. *Proc. Natl. Acad. Sci. U.S.A.* **116**, 10214–10222 (2019).

115 D. A. Davis *et al.*, Force-induced activation of covalent bonds in mechanoresponsive polymeric materials. *Nature* **459**, 68–72 (2009).

116 G. R. Gossweiler *et al.*, Mechanochemical activation of covalent bonds in polymers with full and repeatable macroscopic shape recovery. *ACS Macro Lett.* **3**, 216–219 (2014).

117 A. M. Kushner, V. Gabuchian, E. G. Johnson, Z. Guan, Biomimetic design of reversibly unfolding cross-linker to enhance mechanical properties of 3D network polymers. *J. Am. Chem. Soc.* **129**, 14110–14111 (2007).

118 P. E. Marszalek *et al.*, Mechanical unfolding intermediates in titin modules. *Nature* **402**, 100–103 (1999).

119 S. Tang, B. D. Olsen, Relaxation processes in supramolecular metallogels based on histidine-nickel coordination bonds. *Macromolecules* **49**, 9163–9175 (2016).

120 S. C. Grindy, N. Holten-Andersen, Bio-inspired metal-coordinate hydrogels with programmable viscoelastic material functions controlled by longwave UV light. *Soft Matter* **13**, 4057–4065 (2017).

121 G. A. Parada, X. Zhao, Ideal reversible polymer networks. *Soft Matter* **14**, 5186–5196 (2018).

122 R. Shunmugam, G. J. Gabriel, K. A. Aamer, G. N. Tew, Metal-ligand-containing polymers: Terpyridine as the supramolecular unit. *Macromol. Rapid Commun.* **31**, 784–793 (2010).

123 Y. Zha, M. L. Disabb-Miller, Z. D. Johnson, M. A. Hickner, G. N. Tew, Metal-cation-based anion exchange membranes. *J. Am. Chem. Soc.* **134**, 4493–4496 (2012).

124 M. T. Kwasny, G. N. Tew, Expanding metal cation options in polymeric anion exchange membranes. *J. Mater. Chem.* **5**, 1400–1405 (2017).

Barney et al.